XLIII CILAMCE
21–25, November, 2022
FOZ DO IGUAÇU – PR – BRAZIL

Numerical analysis on pollutant dispersion in naturally ventilated buildings: nonisothermal conditions

Gabriela P. Bianchin[1], Alexandre L. Braun[1]

[1]*Programa de Pós-Graduação em Engenharia Civil (PPGEC), Universidade Federal do Rio Grande do Sul (UFRGS)*
Av. Osvaldo Aranha, 99, 90035-190, Porto Alegre/Rio Grande do Sul, Brasil
gabriela_bianchin@hotmail.com, alexandre.braun@ufrgs.br

Abstract. Pollutants dispersion and human exposure in urban areas are closely linked to urban and building ventilation. In this sense, the main target of the present work is to study the pollutant dispersion phenomenon in naturally ventilated buildings using a numerical model considering incompressible flows with heat and mass transport. For the flow simulation, a semi-implicit Characteristic-Based Split (CBS) model is used in the context of the Finite Element Method, where linear tetrahedral elements are used in spatial discretization. The Navier-Stokes equations and the conservation equations for mass, energy and chemical species form the system of fundamental equations for the flow field. Flow turbulence is treated through Large Eddy Simulation (LES), where the Smagorinsky's approach is adopted for subgrid scale modeling. Thermal effects on the flow field are considered in the momentum balance equation through buoyancy forces, which are calculated taking into account the Boussinesq's approximation. Classic examples of Fluid Dynamics and Transport Phenomena are analyzed to verify the numerical model proposed here and a numerical investigation is performed considering a building model subject to natural ventilation, where pollutant dispersion and thermal effects are evaluated simultaneously.

Keywords: Computational Wind Engineering; Large Eddy Simulation; Natural Ventilation; Heat Transfer; Pollutant Dispersion

1 Introduction

The environmental conditions in urban cities have been constantly deteriorated during the last years owing to the action of pollutant sources such as motor vehicles and building exhaust systems (rooftop stacks) [1]. Rapid urbanization, deteriorating air quality, and air pollutants exposure increase the risks of diseases for residents in urban areas [2,3]. Supply of fresh air with appropriate temperature and humidity is essential for indoor comfort and occupants' health in buildings [4]. In this sense, pollutants dispersion and human exposure in urban areas are closely linked to natural ventilation in buildings, which is the simplest and most economic way to provide sufficient fresh air and achieve indoor thermal comfort [4].

People spend almost 90% of their time in indoor spaces, thus, it is necessary to understand how the outdoor environment affects the indoor air quality of naturally ventilated buildings [5]. Building façades connect indoor and outdoor environments and thus have a considerable regulating effect on indoor environments. Natural ventilation occurs when the vents (such as doors or windows) are open. Most of the studies developed focused in analysis of the ventilation, on pollutant removal properties of street canyons, or the indoor and outdoor pollutant concentration ratios, conducted under isothermal conditions [3, 4, 5]. However, natural ventilation is not only driven by wind but also by buoyancy forces (thermal effects). Therefore, studies are lacking about the influence of outdoor pollutants in street canyons on the indoor air environment, specifically with nonisothermal conditions [3].

In the present work, a numerical model based on the finite element method (FEM) and Large Eddy Simulation (LES) is proposed in order to investigate pollutant dispersion in street canyons, considering a building model subject to natural ventilation, with thermal effects. A finite element model based on the semi-implicit CBS scheme is utilized, where linear tetrahedral elements are adopted for spatial discretization. Two-dimensional simulations are performed to verify the numerical model proposed here, where a LES-type model with adjustment of the Smagorinky's constant is adopted. Although the LES methodology is an inherently three-dimensional approach, a two-dimensional analysis can also be adopted approximately in the case of flows with homogeneous longitudinal fluctuations [6].

2 Equations

2.1 Flow formulation

Some physical assumptions concerning the fluid flow model adopted here are initially presented (see, for instance, Braun and Awruch [7]): natural wind streams are considered to be within the incompressible and turbulent flow range; air is considered mechanically as a Newtonian fluid. In addition, incompressible flows under thermal effects are generally analyzed using the Boussinesq's approximation, where density variations are considered in terms of body forces.

Consequently, the flow fundamental equations are the Navier-Stokes and conservation equations for mass, energy and chemical species. Flow turbulence is resolved using LES and Smagorinsky subgrid-scale modeling (Smagorinsky [8]; Germano et al. [9]; Lilly [10]) as follows:

$$
\begin{aligned}
&\frac{\partial v_i}{\partial t} + v_j \frac{\partial v_i}{\partial x_j} = \frac{1}{\rho}\frac{\partial}{\partial x_j}(\sigma_{ij} + \tau_{ij}^{SGS}) - g_i \beta (T - T_0) \qquad (i, j = 1,2,3) \qquad \text{in } \Omega^{\mathrm{f}} \\
&\frac{\partial v_i}{\partial x_i} = 0 \qquad (i = 1,2,3) \qquad \text{in } \Omega^{\mathrm{f}} \\
&\frac{\partial T}{\partial t} + v_j \frac{\partial T}{\partial x_j} = \frac{1}{\rho c_v}\left(k \frac{\partial^2 T}{\partial x_j^{\,2}} + \rho f_T \right) \qquad (i, j, k = 1,2,3) \qquad \text{in } \Omega^{\mathrm{f}} \\
&\frac{\partial (C_i)}{\partial t} + v_j \frac{\partial (C_i)}{\partial x_j} = D_i \frac{\partial^2 C_i}{\partial x_j^2} + f_{C_i} \qquad (i = 1, n; \quad j = 1,2,3) \qquad \text{in } \Omega^{\mathrm{f}}
\end{aligned}
\tag{1}
$$

In order to solve the flow problem, initial conditions on the flow variables v_i and p must be specified. In addition, appropriate boundary conditions must also be defined on $\Gamma_{\mathrm{t}}^{\mathrm{Tf}}$, which may be expressed as:

$$
\begin{aligned}
&v_i = \bar{v}_i \qquad (i = 1,2,3) \qquad \text{on } \Gamma^{\mathrm{v}} \qquad p = \bar{p} \qquad \text{on } \Gamma^{\mathrm{p}} \\
&T = \bar{T} \qquad \text{on } \Gamma^{\mathrm{T}} \qquad C = \bar{C} \qquad \text{on } \Gamma^{\mathrm{C}} \\
&\sigma_{ij} n_j = \left[-p\delta_{ij} + \tau_{ij} \right] n_j = t_i = \bar{t}_i \qquad (i, j = 1,2,3) \qquad \text{on } \Gamma^{\sigma}
\end{aligned}
\tag{2}
$$

where Γ^{v} (boundary with prescribed velocity $\bar{v}_i$), Γ^{p} (boundary with prescribed pressure $\bar{p}$), Γ^{T} (boundary with prescribed temperature $\bar{T}$), Γ^{C} (boundary with prescribed pollutant dispersion $\bar{C}$) and Γ^{σ} (boundary with prescribed traction $\bar{t}_i$) are complementary subsets of $\Gamma_{\mathrm{t}}^{\mathrm{Tf}}$, such that $\Gamma_{\mathrm{t}}^{\mathrm{Tf}} = \Gamma^{\mathrm{v}} \cup \Gamma^{\mathrm{p}} \cup \Gamma^{C} \cup \Gamma^{T} \cup \Gamma^{\sigma}$. In Eq. (2), n_j are components of the unit normal vector **n** evaluated at a point on boundary Γ^{σ}.

2.2 Numerical Model

The Characteristic-based Split (CBS) scheme is formulated considering a coordinate shift along the flow characteristic directions to remove the advective term from the flow fundamental equations, which permits the use of standard Galerkin procedures in finite element spatial discretizations without the emergence of numerical instabilities. Mesh updating is avoided by using Taylor series approximations in the spatial domain and a split operation is utilized following a numerical procedure proposed initially by Chorin [11] for incompressible flows in a finite difference context. The split operation enables the use of arbitrary interpolation functions for both the

pressure, velocity, energy and pollutant dispersion fields and enhances pressure stability. Additional information on the CBS scheme may be found in Zienkiewicz et al. [12] and Nithiarasu et al. [13]. The standard Galerkin procedure is adopted here for spatial discretization of the flow equations after a temporal discretization operation is accomplished using the CBS scheme, where linear tetrahedral elements are utilized for both the velocity and pressure fields. Viscous and stabilizing terms are integrated by parts in steps 1 and 3, while the pressure Laplacian is integrated by parts in step 2, leading to boundary integral terms. A system of linear algebraic equations is then obtained for the discretized flow equations, which are expressed in matrix form as:

Step 1: intermediate velocity

$$\tilde{\mathbf{v}}_i = \mathbf{v}_i^n - \mathbf{M}_d^{-1}\Delta t\left[\left(\mathbf{A}+\mathbf{D}\right)\mathbf{v}_i - \frac{\Delta t}{2}\mathbf{S}_v - \mathbf{f}_i\right]^n \qquad (i=1,2,3) \tag{3}$$

Step 2: pressure calculation

$$\mathbf{H}\mathbf{p}^{n+1} = \frac{\rho}{\Delta t}\mathbf{G}_i^T\tilde{\mathbf{v}}_i \qquad (i=1,2,3) \tag{4}$$

Step 3: velocity correction

$$\mathbf{v}_i^{n+1} = \tilde{\mathbf{v}}_i - \mathbf{M}_d^{-1}\frac{\Delta t}{\rho}\left[\mathbf{G}_i\mathbf{p}^{n+1} + \frac{\Delta t}{2}\left(\mathbf{S}_p\right)_i\mathbf{p}^n\right] \qquad (i=1,2,3) \tag{5}$$

Step 4: temperature calculation

$$\frac{\Delta\mathbf{T}}{\Delta t} = -\mathbf{M}_d^{-1}\left[\mathbf{A}\mathbf{T}^n + \mathbf{D}\mathbf{T}^n + \frac{\Delta t}{2}\mathbf{S}_v\mathbf{T}^n - \mathbf{f}_T\right] \tag{6}$$

Step 5: concentration of species calculation

$$\frac{\Delta\mathbf{C}}{\Delta t} = -\mathbf{M}_d^{-1}\left[\mathbf{A}\mathbf{C}^n + \mathbf{D}\mathbf{C}^n + \frac{\Delta t}{2}\mathbf{S}_v\mathbf{C}^n - \mathbf{f}_C\right] \tag{7}$$

where $\mathbf{v}_i$ is the flow velocity vector evaluated at nodal level, $\mathbf{p}$, $\mathbf{T}$ and $\mathbf{C}$ are nodal vectors for pressure, temperature and concentration of species, while $\mathbf{M}_d$ is the discrete mass matrix, which is obtained from the consistent mass matrix $\mathbf{M}$.

A global time increment Δt is defined considering instantaneous flow conditions observed at element level, which leads to the following expression:

$$\Delta t = \min\left(\Delta t_{conv}, \Delta t_{dif}, \Delta t_{dif,T}, \Delta t_{dif,C}\right) \quad \text{with} \quad \Delta t_{conv} = \frac{l}{\|\mathbf{v}\|}; \quad \Delta t_{dif} = \frac{l^2}{2Re}; \quad \Delta t_{difT} = \frac{l^2}{2k}; \quad \Delta t_{difC} = \frac{l^2}{2Le} \tag{8}$$

where l is the finite element characteristic length, $\mathbf{v}$ is the vector of nodal velocities at element level, Re is the Reynolds number, Le is the Lewis number and k is the thermal conductivity. A safety coefficient is applied to the global time increment obtained from Eq. (8), which usually ranges from 0.5 to 2 according to mesh characteristics and flow complexity.

3 Numerical Examples

The pollutant dispersion around buildings is simulated here using two-dimensional models of street canyons formed by a pair of buildings with the same height. In the first configuration both buildings are impermeable, while the second configuration shows the upward building subject to natural ventilation. These examples are important because they consider the flow around the buildings, subject to the influence of temperature effects and show how natural ventilation may change the flow and dispersion of pollutants. Results regarding the first configuration analyzed here are presented below and compared with numerical predictions obtained by Madalozzo *et al*. [1] and Madalozzo [14]. Computational domains and boundary conditions adopted in the present analysis are shown in Figure 1, where geometric configurations can be identified with their respective finite element meshes, which are shown in detail for a region around the canyon location. The finite element

meshes are constituted by 890,127 and 951,741 elements for configurations 1 and 2, respectively. The smaller element lengths are located next to the building and ground surfaces, with $\Delta x = 0.002$ m. The pollutant is emitted from a point source positioned at the bottom of the canyons with emission rate of $S_P = 0.01$ m^3/s. The flow properties utilized in the present simulations are characterized by the following dimensionless numbers: *Re* = 10^4, *Sc* and $Sc_t = 0.72$, *Ri* = -0.2 (*Richardson number*) and the Smagorinsky's constant C_s is set to 0.12 when the classical model is employed.

In addition, two cases were also simulated considering the building configurations utilized in the present study. In the first case (case 0), the ground and building surfaces are heated, while the second case (case 1) considers the sun shining from the upper left corner of the computational domain, which leads to partial heating of the ground and buildings walls. The third (case 2) and fourth (case 3) cases are equivalent to the second test, where openings are considered, as indicated in Figure 1. Case 2 has both the windows open, while case 3 shows that only the leeward opening is open. For these cases the ground and building walls are heated. The numerical simulations were performed up to t = 15 s and time average fields were obtained over the last 5 s of the present analyses, as indicated by Madalozzo [14].

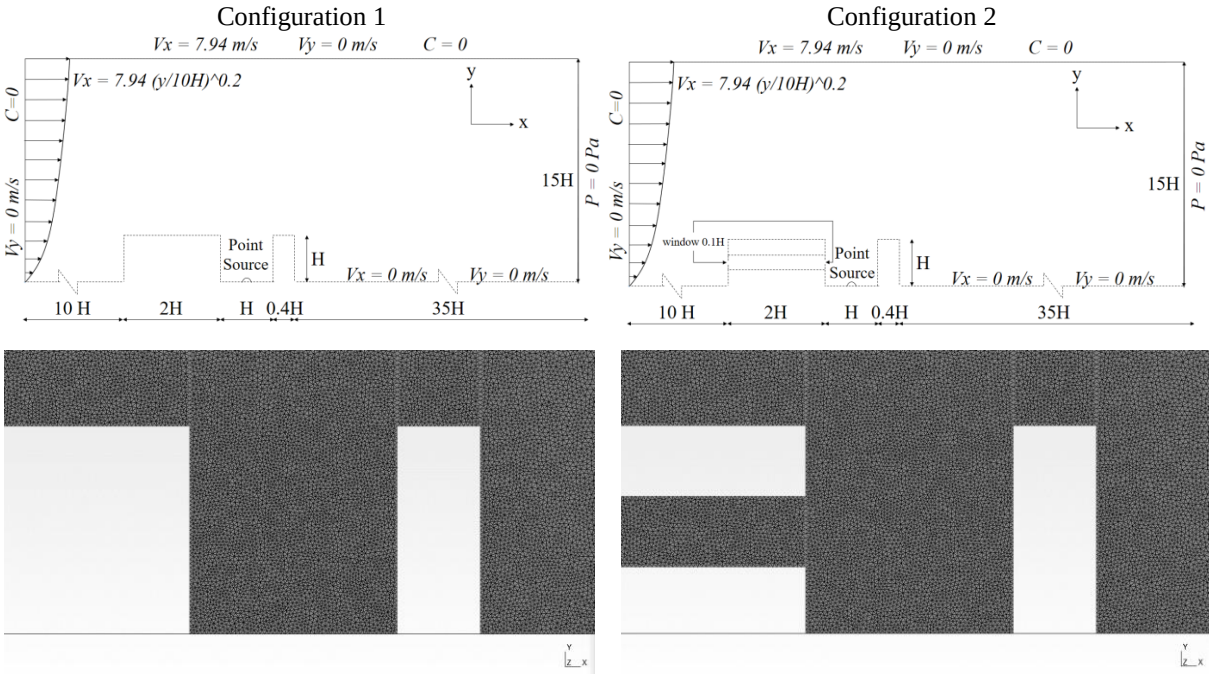

Figure 1. Two-dimensional buildings analysis: computational domain and finite element mesh

Figure 2 presents distributions of the velocity components v_x and v_y along the height and measured in the center of the street canyon formed by the two buildings (y = 0.5 and x = 12.5, respectively). The comparison with the results obtained by Madalozzo [14] indicates excellent approximations for cases 0 and 1. The concentration of pollutants is shown on the leeward wall of the first building, on the windward wall of the second building and in the bottom of the cavity formed by them. Configuration 1 is in agreement with the results obtained for street canyons with unit aspect ratio (see Madalozzo et al. [14]).

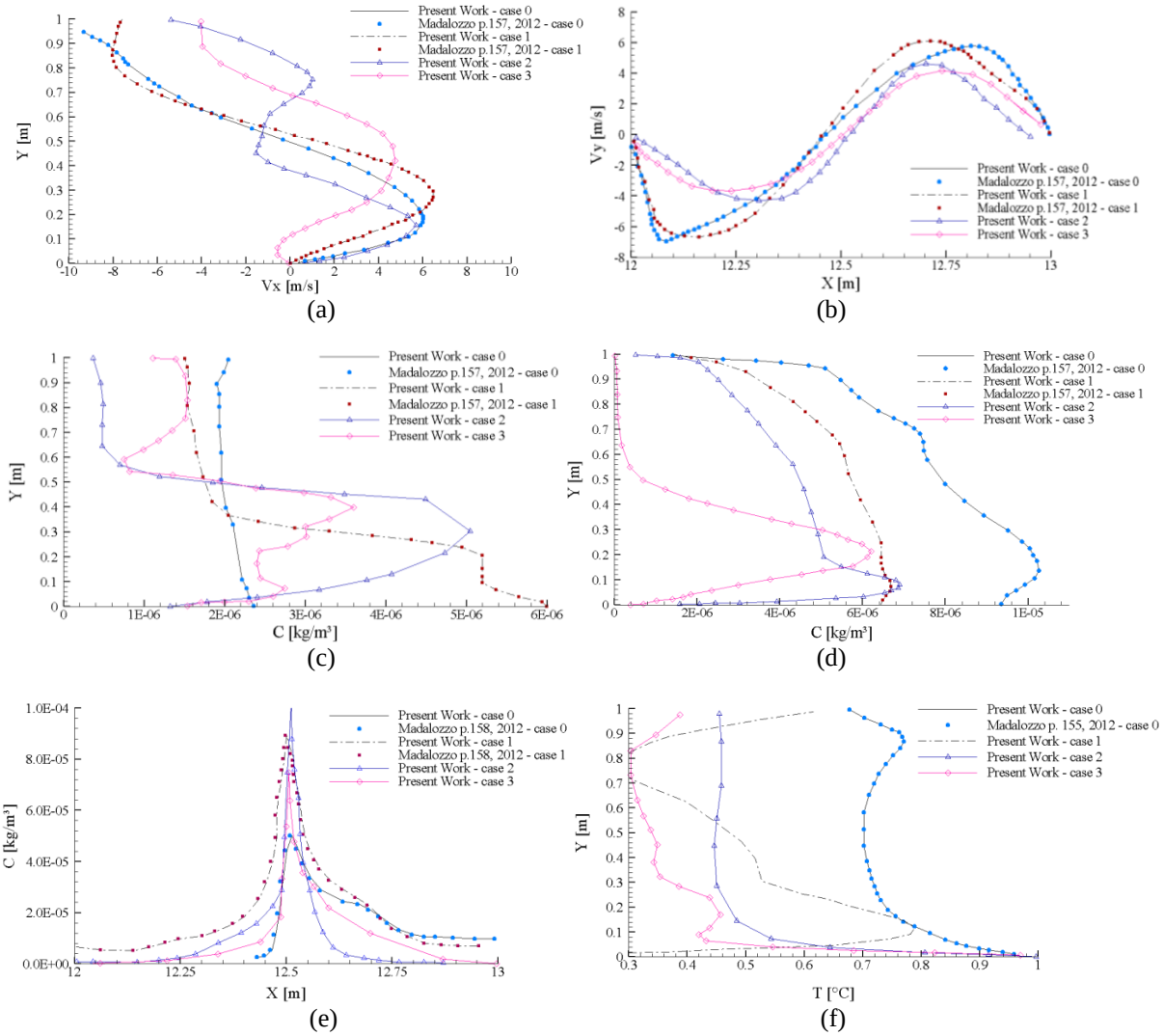

Figure 2. Two-dimensional buildings analysis: (a) flow velocity component v_x; (b) flow velocity component v_y; (c) pollutant concentration along the wall of the upstream building; (d) pollutant concentration along the wall of the downstream building; (e) pollutant concentration along the bottom of the canyon; (f) temperature distribution along height

The distribution of pollutants in the canyon cavity also follows the same characteristics observed by Madalozzo [14]. Due to the flow pattern, the pollutant concentration is stronger for a region close to the side wall of the first building and the pollutant removal is more efficient for cases 2 and 3. Figure 3a presents the time average streamlines obtained with the numerical model proposed in this work for the different configurations investigated. One can notice that a circulation zone due to flow separation is observed above the upstream building, which reattaches before the corresponding trailing edge. Consequently, a clockwise recirculation zone is produced in the present simulations. Temperature time-mean scalar fields are shown here for the four proposed configurations.

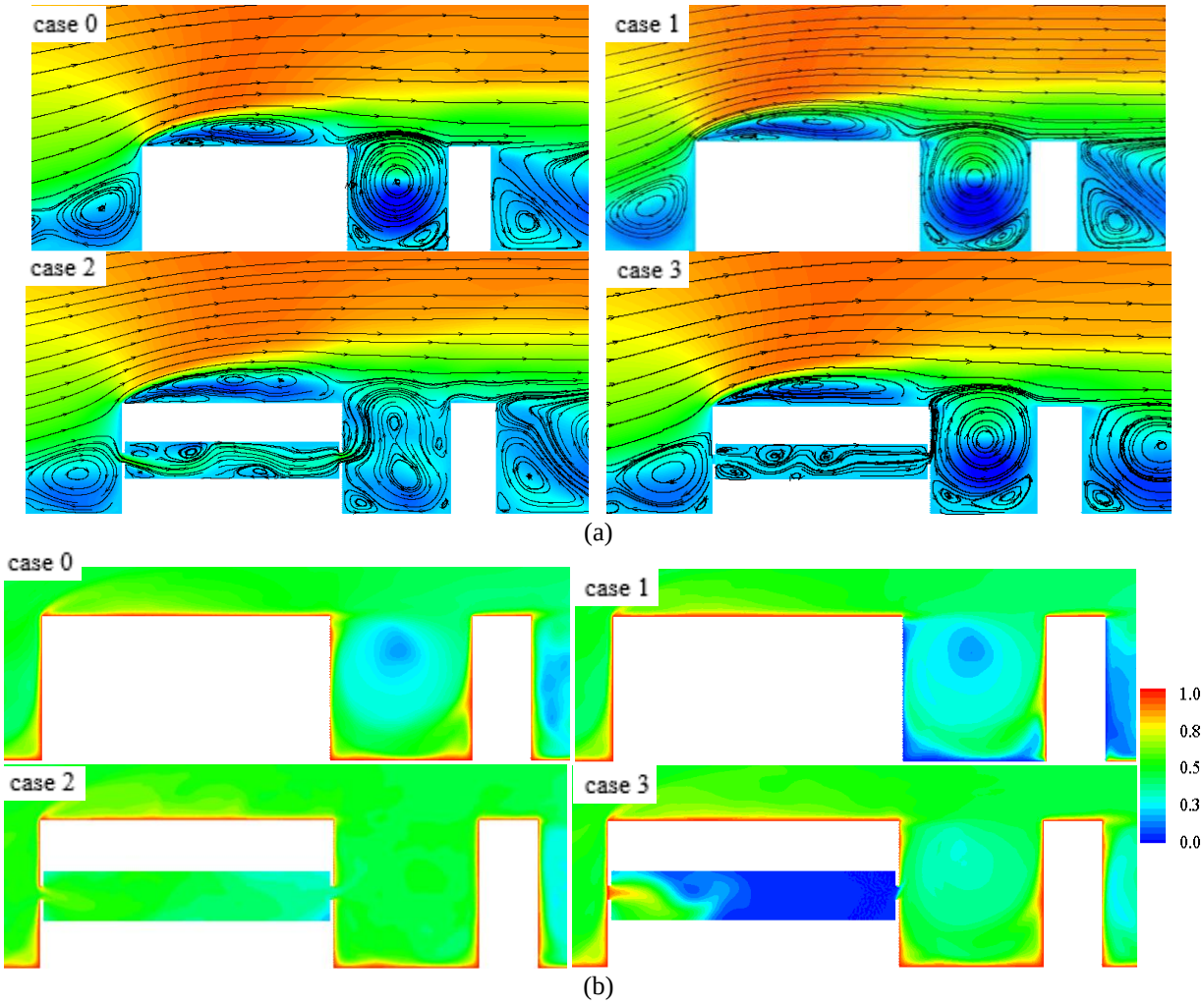

Figure 3. Two-dimensional buildings analysis: (a) time average streamlines; (b) isotherms

Note that case 2 has a great potential for minimizing the thermal effect by considering the natural ventilation of the building, even in the street canyon, while case 3 causes unwanted internal heating. In this way, natural ventilation is not only driven by the wind, but also by buoyancy forces (due to thermal effects), contributing to the improvement of air quality inside buildings and street canyons.

4 Conclusions

A numerical investigation was proposed in this work to evaluate the influence of temperature effects on pollutant dispersion in street canyons, considering a building model subject to natural ventilation. Some applications involving fluid dynamics and transport phenomena were analyzed to verify the numerical model proposed here, whose results were compared with the predictions obtained by Madalozzo [14]. A good approximation was obtained for the cases studied here. Natural cross ventilation (case 2) improved pollutant dispersion and temperature distribution both inside the building and in the street canyon formed between the two buildings simulated here. On the other hand, buildings without ventilation (cases 0 and 1) and case 3, with a single opening, made these processes difficult. In this sense, it is understood that natural ventilation has potential to minimize the impacts of high temperatures and dispersion of pollutants in urban areas.

Acknowledgements. The authors would like to thank the National Council for Scientific and Technological Development (CNPq, Brazil) and the Brazilian Federal Agency for Support and Evaluation of Graduate

Education (CAPES, Brazil) for the financial support. The present research was developed using computational resources provided by the High Performance Computing Center (NACAD/UFRJ, Brazil).

Authorship statement. The authors hereby confirm that they are the sole liable persons responsible for the authorship of this work, and that all material that has been herein included as part of the present paper is either the property (and authorship) of the authors, or has the permission of the owners to be included here.

References

[1] D.M.S. Madalozzo, A.L. Braun, A.M.Awruch, I.B. Morsch, Numerical simulation of pollutant dispersion in street canyons: Geometric and thermal effects, Applied Mathematical Modelling, 38 (2014) 5883-5909.
[2] S.J. Mei, C.W. Liu, D. Liub, F.Y. Zhao, H.Q. Wang, X.H. Li, Fluid mechanical dispersion of airborne pollutants inside urban street canyons subjecting to multi-component ventilation and unstable thermal stratifications, Science of the Total Environment, 565 (2016) 1102-1115.
[3] Y. Hu, Y. Wu, Q. Wang, J. Hang, Q. Li, J. Liang, H. Ling, X. Zhang, Impact of Indoor-Outdoor Temperature Difference on Building Ventilation and Pollutant Dispersion within Urban Communities, Atmosphere, 13 (2022).
[4] F. Yang, Y. Kang, Y. Gao, K. Zhong, Numerical simulations of the effect of outdoor pollutants on indoor air quality of buildings next to a street canyon, Building and Environment, 87 (2015) 10-22.
[5] Y. Xiong, H. Chen, Effects of sunshields on vehicular pollutant dispersion and indoor air quality: Comparison between isothermal and nonisothermal conditions, Building and Environment, 198 (2021) 107854.
[6] L. Bruno, S. Khris. The validity of 2D numerical simulations of vertical structures around a bridge deck, Math. Comput. Model, 37 (2003) 795-828.
[7] A.L. Braun, A.M. Awruch, Aerodynamic and aeroelastic analyses on the CAARC standard tall building model using numerical simulation, Computers and Structures 87(9-10) (2009) 564-581.
[8] J. Smagorinsky, General circulation experiments with the primitive equations, I, the basic experiment, Monthly Weather Review 91 (1963) 99-135.
[9] M. Germano, U. Piomelli, P. Moin, W.H. Cabot, A dynamic subgrid-scale eddy viscosity model, Physics of Fluids 3 (1991) 1760-1765.
[10] D.K. Lilly, A proposed modification of the Germano subgrid-scale closure method, Physics of Fluids 4 (1992) 633-635.
[11] A.J. Chorin, Numerical solution of Navier-Stokes equations, Mathematics of Computation 22 (1968) 745 –762.
[12] O.C. Zienkiewicz, R.L. Taylor, P. Nithiarasu, The Finite Element Method for Fluid Dynamics, 7th ed., Butterworth-Heinemann, Waltham, 2013.
[13] P. Nithiarasu, R.W. Lewis, K.N. Seetharamu, Fundamentals of the Finite Element Method for Heat and Mass Transfer, 2nd ed., Wiley, Chichester, West Sussex, 2016.
[14] D. M. S. Madalozzo, Simulação Numérica da Dispersão de Poluentes em Zonas Urbanas Considerando Efeitos Térmicos, 2012. Dissertação (Mestrado) – Programa de Pós-Graduação em Engenharia Civil, UFRGS, Porto Alegre.